Electronic Supplementary Material (ESI) for Physical Chemistry Chemical Physics.
This journal is © the Owner Societies 2020

# *In cell* $Gd^{3+}$-based site-directed spin labeling and EPR spectroscopy of eGFP

Svetlana Kucher[a], Sergej Korneev[b], Johann P. Klare*[a], Daniel Klose*[c], Heinz-Jürgen Steinhoff*[a]

[a]Department of Physics, Osnabrück University, Barbarastr. 7, Osnabrück, Germany

present address (S. Kucher): Faculty of Chemistry and Biochemistry, Ruhr University Bochum, Universitaetsstr. 150, Bochum, Germany

[b]Department of Biology, Osnabrück University, Barbarastr. 11, Osnabrück, Germany

[c]Department of Chemistry and Applied Biosciences, ETH Zurich, Vladimir-Prelog-Weg 2, Zurich, Switzerland

*Corresponding authors. E-mail addresses:

hsteinho@uni-osnabrueck.de

daniel.klose@phys.chem.ethz.ch

jklare@uos.de

**Contents**

**SI 1 Synthesis of DOTAM-azide and complexation with $Gd^{3+}$**

Starting compounds and solvents were purchased from the appropriate suppliers and were used as obtained. Reactions were carried out under Ar in a dry Schlenk flask. Unstabilized solvents $CH_2Cl_2$ (SeccoSolv, Merck, Germany), acetonitrile (Sigma-Aldrich, Germany) and MeOH (Fisher Scientific, Germany) of dry grade packed under nitrogen were used for reactions. Column chromatography: silica gel 60 ($SiO_2$; Merck, Germany), TLC: aluminum plates, $SiO_2$ 60 $F_{254}$, 0.2-mm layer (Merck, Germany). NMR Spectra: AMX-500 spectrometer (Bruker, Rheinstetten, Germany); $^1$H: 500.14, $^{13}$C: 125.76, in ppm rel. to the signals of the residual protons of $CHCl_3$ ($\delta$ =7.26 ppm) in $CDCl_3$ or $CH_3OH$ ($\delta$ = 3.35 ppm) in $CD_3OD$, carbons of $CDCl_3$ ($\delta$ =77.00 ppm) or $CD_3OD$ ($\delta$ = 49.3 ppm). ESI-MS: Bruker Daltonics Esquire HCT instrument (Bruker Daltonics, Bremen, Germany); ionization was performed with a 2% aq. HCOOH solution. Elemental analyses (C, H, N): VarioMICRO instrument (Fa. Elementar, Hanau, Germany).

*N-(3-Azidopropyl)-2-bromoacetamide (**2**)*

A solution of 3-azidopropylamine (100 mg, 1 mmol), prepared from 3-cloropropylamine hydrochloride and sodium azide in $H_2O$ according to [1], and triethylamine (111 mg, 1.1 mmol) in $CH_2Cl_2$ (1 ml) was added dropwise to a pre-cooled (ice-bath) solution of bromoacetyl chloride (173 mg, 1.1 mmol) in $CH_2Cl_2$ (1 ml) and the resulting mixture was stirred overnight (see Scheme S1). It was diluted with $CH_2Cl_2$ (4 ml), washed consecutively with $H_2O$ (3 x 3 ml) and saturated aq. $NaHCO_3$, dried ($Na_2SO_4$) and concentrated. The colorless oily residue was chromatographed over $SiO_2$ (eluted with $CH_2Cl_2$-AcOEt, 9:1 v/v mixture) to give 77.3 mg (70%) of azidoamide **2** as colorless oil. TLC ($CH_2Cl_2$:AcOH, 8:1 v/v): $R_f$ 0.52. $^1$H NMR ($CDCl_3$): 6.68 (1H, br s, NH), 3.87 (2H, s, $CH_2Br$), 3.43-3.38 (4H, m, 2 x $CH_2N$ 1.80 (2H, qnt, $J$ 6.6, $CH_2$). $^{13}$C NMR ($CDCl_3$): 165.56 (C=O), 49.32 ($CN_3$), 37.93 (CN), 29.09 (CBr), 28.53 ($CH_2$). NMR spectral data are in good agreement with those reported. [2]

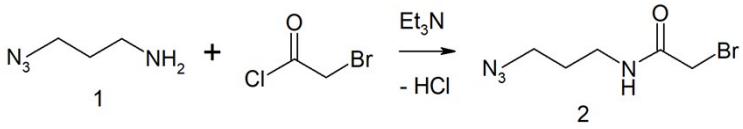


**Scheme S1**. Synthesis of *N-(3-Azidopropyl)-2-bromoacetamide (**2**).*

*N-(3-Azidopropyl)-1,4,7,10-tetraazacyclododecane-1,4,7,10-tetraacetamide (**3**)*

Powdered $K_2CO_3$ (55 mg, 0.4 mole, anhydrous) and 1,4,7,10-tetraazacyclododecane-1,4,7-triacetamide (68.6 mg, 0.2 mole 97%, CheMatech) were added consecutively to a solution of azidoamide **2** (200 mg, 0.3 mole) in MeOH (2 ml) and the resulting white suspension was stirred at 55˚C overnight (see Scheme S2). The reaction mixture was concentrated, the residue was suspended in acetonitrile (5 ml, 99.9%), white precipitate was separated and washed with acetonitrile (3 x 1 ml). The combined filtrates were concentrated and resuspended in $CH_2Cl_2$ (2 ml), beige precipitate was separated and washed with $CH_2Cl_2$ (3 x 1 ml) to give 41.3 mg (42 %) of DOTAM-azide **3** as light-beige powder. TLC ($CH_2Cl_2$: MeOH, 4:1 v/v): $R_f$ 0.57. $^1$H NMR ($CD_3OD$): 3.35 (2H, t, $J$ 6.8, $CH_2N_3$), 3.29 (4H, s), 3.26 (2H, t, $J$ 6.8, $CH_2N$), 2.80 (10H, br s, $CH_{2\ cycl}$), 2.10 (6H, br s, $CH_2CO$), 1.74 (2H, qnt, $J$ 6.8, $CH_2$) is shown in Fig. S1 A. $^{13}$C NMR ($CD_3OD$): 174.65, 174.61, 172.85, 171.85 (C=O), 57.65 ($NCH_2O$), 56.88 (3 x $NCH_2O$), 50.63 (br, 6 x $CH_{2\ cycl}$), 48.72 ($CN_3$), 36.16 (CNH), 28.38 ($CH_2$) is shown in Fig. S1 B. ESI MS (positive mode): 484.5 $[M+1]^+$, 522.5 $[M+39]^+$, HRMS calculated for $[MH]^+$: 484.31081, found: 484.31061, M.p. > 172 $^o$C (decomp).

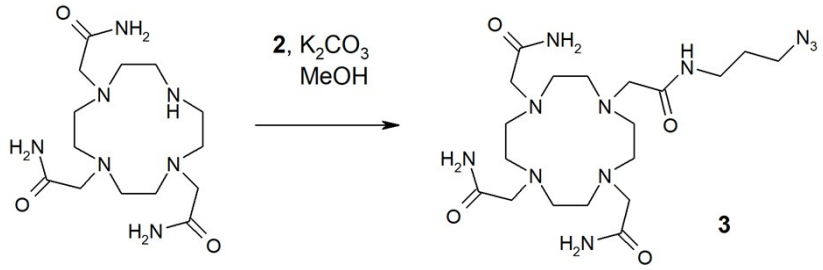


**Scheme S2**. Synthesis of *N-(3-Azidopropyl)-1,4,7,10-tetraazacyclododecane-1,4,7,10-tetraacetamide (**3**).*

**A**

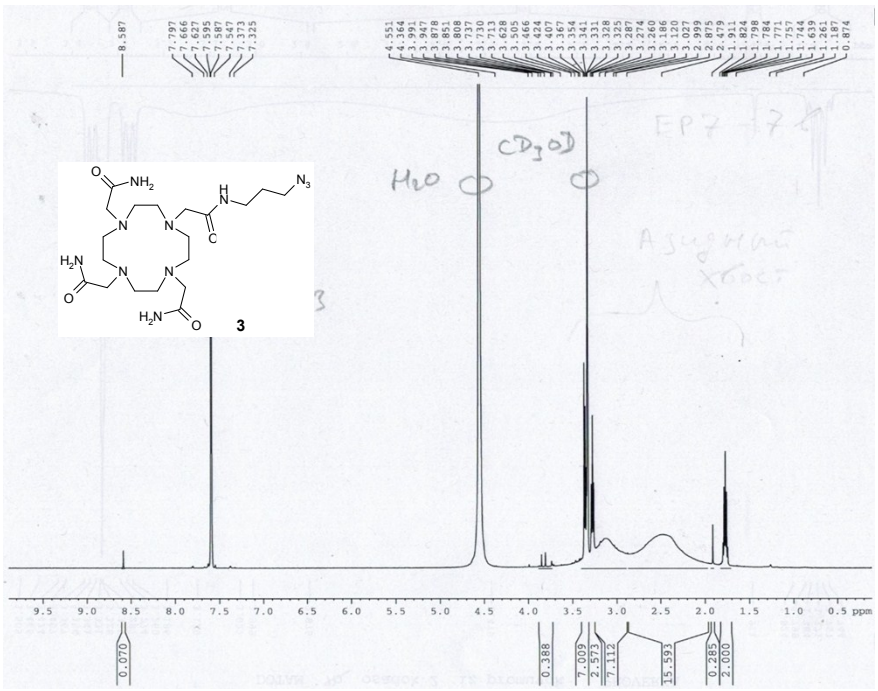


**B**

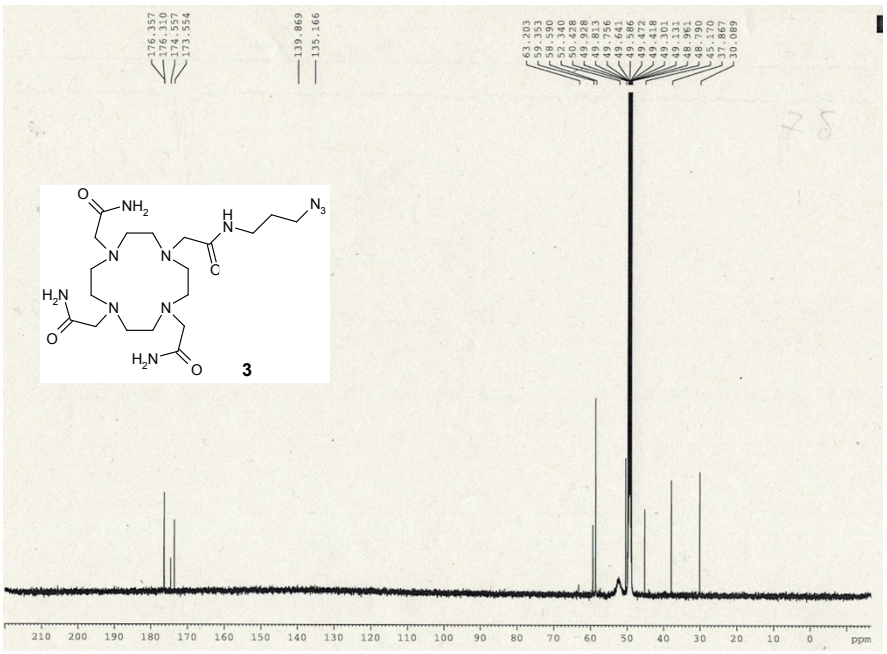


**Figure S1**. **A**: $^{1}$H-NMR (500 MHz, $CD_3OD$) of DOTAM-azide (**3**) and **B**: $^{13}$C-NMR (125 MHz, $CD_3OD$) of DOTAM-azide (**3**).

For the complexation of $Gd^{3+}$ with chelators, first 150 mM stock solutions of $GdCl_3$ (Sigma Aldrich, Germany) and the chelators DOTA(M) (Chematech, France), azido-DOTA(M) (Macrocyclics, USA) were prepared in MOPS buffer (500 mM MOPS, 500 mM NaCl, 10% v/v Gly, pH 6.8) and the final pH was readjusted to 6.8 with NaOH. Then, the solutions were mixed in a ratio 1-1.1:1 (Gd to chelator) and incubated overnight in the dark while shaking at room temperature. The complexation yield was quantified using a xylenol orange test according to protocol given in [3]. The dissociation constants for both DOTA and DOTAM were found to be reasonable high, 24.7 and 14.5,[4] respectively. After all, remaining free gadolinium was chelated by quantitative addition of EDTA to the solution in order to prevent its toxicity.[5]

**SI 2 EPR experimental setup**

Continuous wave (cw) EPR spectra were recorded at room temperature on a Magnettech Miniscope MS300 X-band EPR spectrometer (Magnettech, Germany) equipped with a rectangular resonator TE102 or on home-built spectrometer equipped with a

Bruker MD5 dielectric resonator (Bruker Biospin, Rheinstetten, Germany). 20 µL of samples were placed in 0.9 mm outer diameter glass capillaries and measured with 1-10 mW microwave power and 100 kHz magnetic field modulation. The modulation amplitude was chosen to be maximal 1/3 of the spectral linewidth to avoid line distortion.

Labeling efficiency was determined as the percent ratio between the spin-labeled and total protein concentration. The first was calculated from the comparison of the double integral of cw EPR spectrum with respect to a standard stock solution. 100 µM of GDM was used as a standard for determination of GDMA-labeled samples, 1 mM of Gd-DOTA for DOTA-derivatives and 100 µM Tempol for nitroxides. The error in labeling efficiency determination was estimated statistically to be ±10%.

Distance measurements were performed on an Elexsys E580 Q-band spectrometer (Bruker Biospin, Rheinstetten, Germany) equipped with a 150 W TWT amplifier and a homebuilt TE102 rectangular resonator at Q-band (~34.5 GHz) at 10 K using the four-pulse DEER sequence [6,7]. Samples were mixed with 40% v/v glycerol to a final volume of 40 µL, filled into 3 mm outer diameter quartz tubes and shock-frozen in liquid nitrogen. All pulse lengths were set to 12 ns. Proton nuclear modulations were suppressed by incrementing the first inter pulse delay in 8 steps of 2 ns [14]. The pump pulse was set to the maximum of the nitroxide absorption spectrum and the observer pulses to the maximum of the Gd spectrum as described in [8] allowing the suppression of the distance contributions between the nitroxides (C48R1 and C70R1 in our case) in the obtained experimental distance distribution.

**SI 3 *In vitro* sample preparation**

The recombinant expression of eGFP using the Amber codon suppression strategy for incorporation of the non-canonical amino acid SCO (SiChem, Germany) and purification via Ni-NTA chromatography is described in detail in [9]. The concentration of eGFP was calculated from the UV/Vis absorption spectrum recorded on a UV-2450 spectrophotometer (Shimadzu, Duisburg, Germany) at 490 nm using an extinction coefficient of 55000 $M^{-1}$ $cm^{-1}$.[10] The single and double labeled *in vitro* variants of eGFP-Y39SCO were prepared as described below.

160 µM eGFP-Y39SCO was incubated first with 4 mM $Gd^{3+}$-DOTA(M)-azide (GDA, GDMA) for 4 hours at 37°C, then non-bound spin label was washed out and eGFP was concentrated using Vivaspin 500 concentrators (Sartorius, Germany) with a 10 kDa molecular weight cutoff. For DEER measurements, eGFP-Y39SCO*GDMA was additionally labeled with MTSSL at the native cysteine positions 48 and 70, where the latter one is known to have a low labeling probability.[9] Briefly, eGFP-Y39SCO*GDMA was first incubated with 1mM TCEP (Carl Roth, Germany) for 1 hour at room temperature and subsequently with 5 mM MTSSL for 24 hours. The overall labeling efficiency was calculated to be ~120% for all three labels, mostly due to the low probability of labeling C70.

To monitor the viscosity dependence of $Gd^{3+}$-DOTAM, stock solutions of 1 mM containing different concentrations of glycerol were prepared and cw EPR spectra were recorded at ambient temperature. The Glycerol concentration was calculated into corresponding viscosity units based on the values found in [11]. As viscosity can also be changed by variation of the temperature, which allows to access a higher viscosity range, 40 µM of newly synthesized $Gd^{3+}$-DOTAM-azide in water/glycerol mixtures was measured at different temperatures.

To test CuAAC, eGFP was expressed with unnatural amino acid PrK (SiChem, Germany) instead of SCO. CuAAC labeling of 20 µM of eGFP-Y39PrK with 1mM GDMA using 1mM $CuSO_4$, complexed by 3mM THPTA and reduced by 1 mM NaAsc was not successful. To reduce possible competition between positively charged $Cu^{2+}$ and $Gd^{3+}$ ions, the labeling reaction was carried out with lower copper concentration. Thus, overnight labeling at RT using 300 µM CuSO4, complexed by 900µM THPTA and reduced by 2.5 mM NaAsc, 1 mM GDMA and 20 µM of eGFP-Y39PrK resulted in a spectrum shown in Fig. S2 with a shape similar to eGFP-Y39SCO*GDMA and labeling efficiency of 30%.

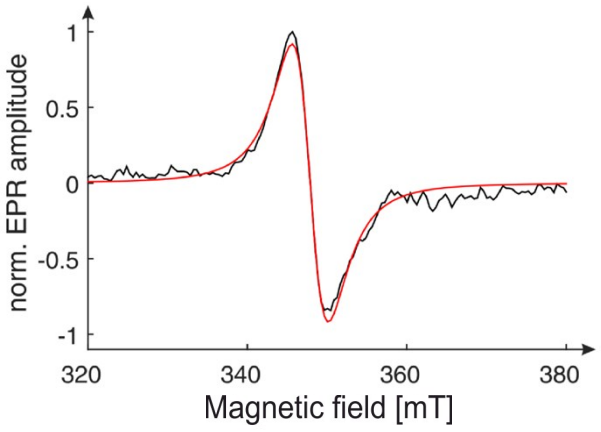


**Figure S2**. RT cw EPR spectrum of eGFP-Y39PrK*GDMA (black). The single Lorentzian is shown in red.

**SI 4 Viscosity dependence of $Gd^{3+}$ complexes**

Fig. S3 A shows the room temperature viscosity dependence of $Gd^{3+}$-DOTAM and $Gd^{3+}$-DOTAM-azide in the 1-34 cp range. The plotted inverse linewidth over the viscosity dependence (main text, Fig. 1 B) agrees with the previously found values for $Gd^{3+}$-DOTAM complex.

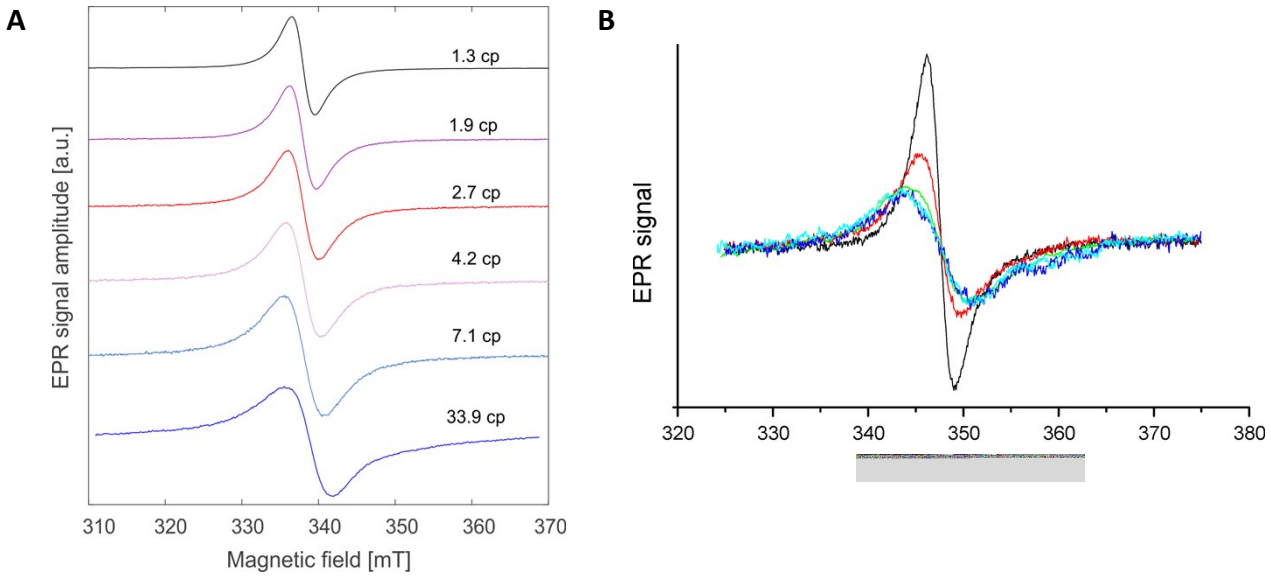


**Figure S3**. Viscosity dependencies of cw EPR spectra of **A**: 1 mM $Gd^{3+}$-DOTAM obtained by variation of glycerol concentration (amplitude-normalized) and **B**: 40 µM $Gd^{3+}$-DOTAM-azide determined in glycerin/water solutions of different concentrations (w/w) and temperatures.

**SI 5 Rotamer library modeling of SCO*$Gd^{3+}$-DOTAM-azide**

The molecular geometry of the complete side chain SCO*$Gd^{3+}$-DOTAM-azide was drawn in 3D using the open source molecular editor Avogadro [12], in which also the subsequent initial geometry optimization was carried out using the universal force field (UFF)[13]. The resulting structure was further geometry optimized by density functional theory (DFT) calculations in Orca 3.0.3[14] using the spin-unrestricted Kohn-Sham formalism with the zero order regular approximation (ZORA)[15] as a relativistic correction and the generalized gradient approximation exchange-correlation functional BP86 and the triple valence basis set TZV-ZORA. The optimized structure was used for Monte Carlo sampling using the eleven rotatable dihedral angles shown in Fig. S4 A as the relevant degrees of freedom. For Monte Carlo sampling only the dihedral angle potentials and the van der Waals energy were considered, both using the UFF[13] for parameterization; for the van der Waals potentials a softening "forgive factor" of 0.8 was chosen [16]. The resulting Monte Carlo ensemble of 250,000 members was clustered further into a representative subset of rotamers using hierarchical clustering in Matlab (Mathworks, Inc.) with the distance in the eleven-dimensional dihedral angle space as the distance metric for the clustering algorithm. Based on comparison of the dihedral angle histograms of the resulting libraries with the whole Monte Carlo ensemble (Fig. S4 B), we chose 8192 rotamers as the required rotamer library size. This rotamer library was integrated into the software *Multiscale Molecular Modeling* (MMM[17]), which allowed us to calculate interspin distance distributions using the graphical user interface according to standard procedures[17] with the new rotamer library with label code GM1 prepared above for SCO*$Gd^{3+}$-DOTAM and the standard MTSSL rotamer library (R1A_298K_UFF_216_r1_CASD, 298 K calibration) for the cysteines C48 and C70. The SCO*$Gd^{3+}$-DOTAM rotamer library is automatically downloaded upon first use within MMM from version 2019.1 (www.epr.ethz.ch → Software). The SCO*$Gd^{3+}$-DOTAM-labeled side chain is designated as GM1.

*In silico* spin labeling of the eGFP X-ray crystal structure (PDB 4EUL[18]) with MTSSL only found a single rotamer populated for both C48 and C70 predominantly due to clashes of the label with the fixed protein backbone of the neighboring loops. Previously, we found[9] that position C70 was barely labeled by MTSSL under these conditions, while position C48 was labeled with quantitative yields. Hence for C70 the single rotamer model may be representative for the experimental result, yet for position C48 this modeling approach reveals stronger local restrictions compared to what we observe experimentally. In order to model an increased local flexibility and possible local loop rearrangement around position C48, we deleted the loop residues 50 to 55 as well as the side chain of residue 216 (Fig. S5). In the subsequent rotamer analysis on this deletion variant, 70 conformations for C48R1 were found to be populated, for all of which the spin label pointed towards the interior of the eGFP barrel, we refer to this as the inner conformation of the spin label. The other two positions, C70 and Y39 remained unaffected by these deletions. The resulting inter spin distance distributions of the C48R1 inner conformation to Y39*GM1 is shown in Fig. 2B (blue). The low experimental degree of labeling for C70R1 is consistent with minor distance contributions in the range of 2 to 2.8 nm in the experimental DEER distance distribution (Fig. S6). The distance Y39*GM1 to C48R1 in contrast explains a major part of the experimentally observed distribution (Fig. S6, Fig. 2B (blue), inner conformation).

Thus far the modeling neglected any backbone flexibility of the residue Cys48, and visual inspection indicated that the spin label C48R1 can be oriented towards the exterior of the eGFP barrel by mere side chain dihedral rotations without distorting the local backbone. We tested this hypothesis by a molecular dynamics simulation of the full (no deletions) eGFP C48R1 variant starting with C48R1 in the inner conformation, i.e. pointing into the eGFP barrel. The protein was immersed in a TIP3P water box with 15 Å padding to all sides and with periodic boundaries, charges were neutralized using $Na^+$ and $Cl^-$ ions at a concentration of 150 mM using VMD[19] and NAMD[20] using the CHARMM36 force field[21] with parameters for the eGFP chromophore[22] and the spin-labeled side chain R1[23]. We employed two stages of each 10,000 steps of conjugate gradient energy minimization, first for the solvent and second also including the protein side chains. Subsequently, we equilibrated the temperature to 293 K using a Langevin thermostat and the pressure to 1 atm

using a Langevin-Piston barostat, in two steps of each 0.5 ns. The backbone atoms were kept fixed for equilibration, after which the flexible loop regions surrounding the labeling site C48 studied here were released, namely residues 48 to 56 and 210 to 216 (Fig. S5). The molecular dynamics of the equilibrated system were simulated at 1 atm constant pressure and at a temperature of 293 K for 10 ns for the initial spin label conformation (rotamer with highest population found by MMM above), which pointed towards the interior of the eGFP-β-barrel. We found that this conformation remained stable, no transitions between canonical dihedral states were observed for the five dihedrals of the spin label. Subsequently, we induced the transition to move the spin label outwards, solely by applying a 10 kT deep harmonic potential for 1 ns on the X3 dihedral angle that changed its value from ca. +90° to -90°. In the following 10 ns long simulation, X3 remained stable around -90° and the spin label continuously pointed outwards with minimal rearrangement of the surrounding loops (0.87 Å root mean square deviation measured over the backbone atoms of residues 48 to 56 and 210 to 216). Since sampling of the R1 degrees of freedom in explicit water requires considerable simulation times[24], we instead used the final coordinates of the second 10 ns-simulation to perform a rotamer analysis in MMM (as described above) for all labeling sites, namely C48R1, C70R1 and Y39GM1; here for C70R1 no populated rotamer was found. The results of this rotamer analysis are given in Fig. 2B as the "outer conformation" (green).

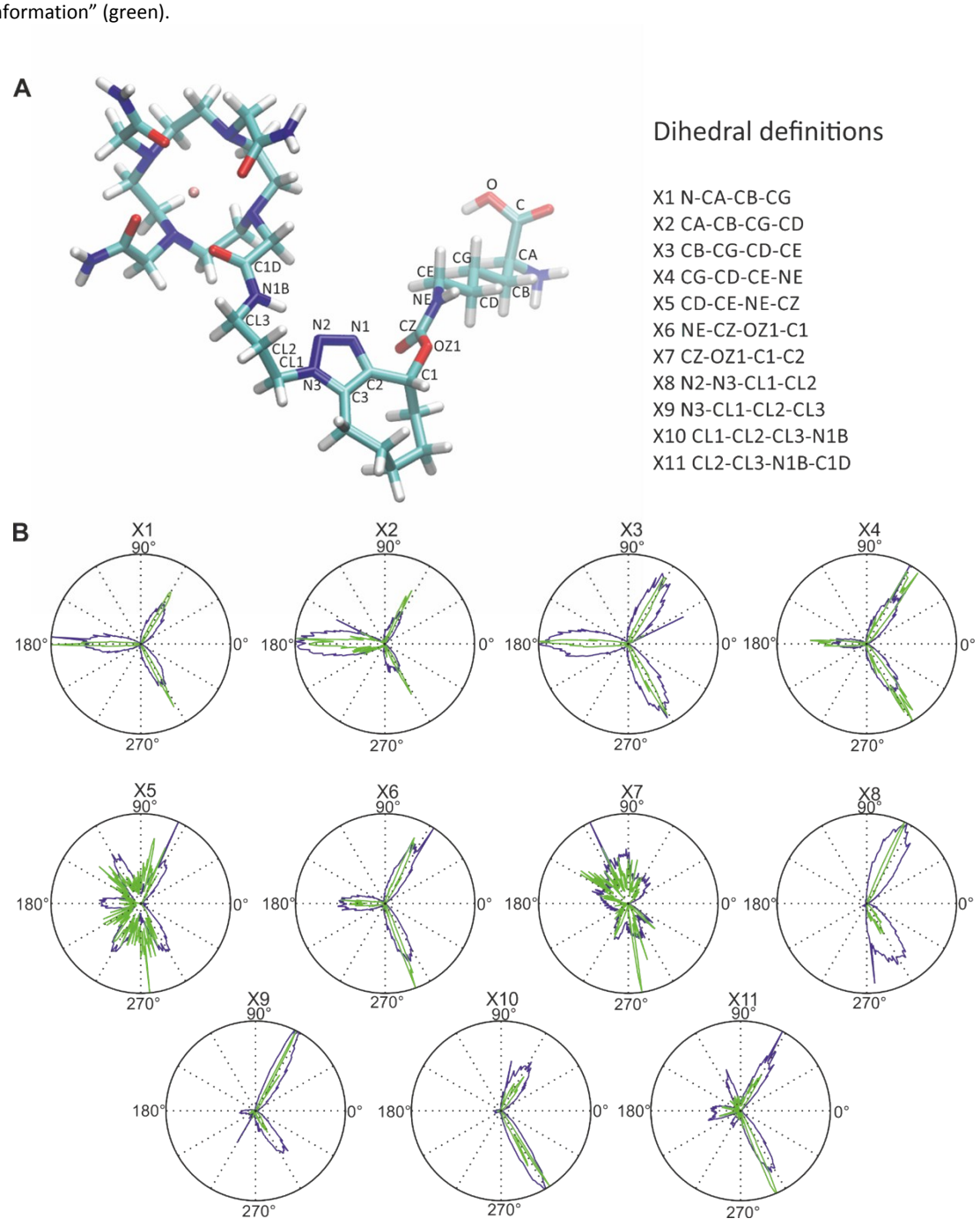


**Figure S4**. Rotamer library generation for SCO-$Gd^{3+}$DOTAM-azide. **A** DFT-optimized structure of the spin-labeled side chain and definitions of the eleven rotatable dihedral angles. **B** Dihedral angle histograms of the eleven dihedral angles, X1 to X11, showing the Monte Carlo ensemble (blue) with 250,000 structures and the 8192-membered rotamer library (green). Canonical dihedral angles found in the Monte Carlo ensemble are in general well represented in the rotamer library, however, two dihedrals (X5 and X7) show averaging between canonical states due to the finite library size.

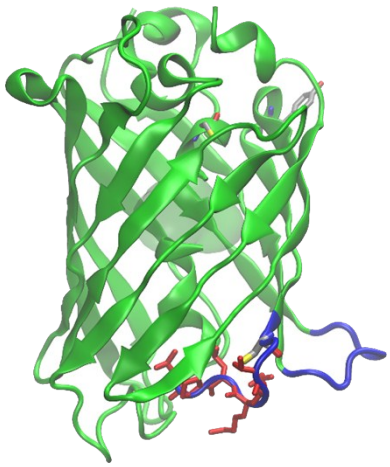

**Figure S5.** Labeling positions and local structure around eGFP C48. Side chains Y39, C48 and C70 are shown in stick representation (carbon gray, oxygen red, nitrogen blue and sulphur yellow). eGFP loop residues 50 to 55 and the side chain 216 (red stick representation) were deleted from the eGFP structure (green ribbon representation, PDB 4EUL) in order to model an increased local flexibility for the rotamer analysis of C48R1. During the molecular dynamics simulations, the loop residues 48 to 56 and 210 to 216 (blue ribbon representation) were unrestrained.

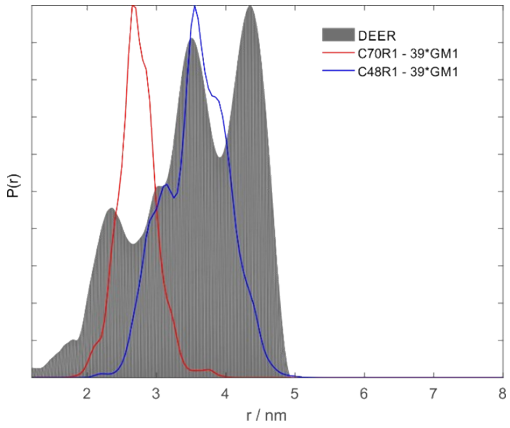


**Figure S6.** Rotamer analysis of eGFP compared to the experimental DEER distance distribution (gray, see also Fig. S8). The simulated distance distribution (blue) by the rotamer analysis of C48R1 in the inner conformation using eGFP (PDB 4EUL) with surrounding loop deletions (Fig. S5 and SI text) to Y39*SCO-$Gd^{3+}$-DOTAM (label termed GM1 in MMM) explains a major part of the experimental distance distribution, while the simulated distribution (red) of label C70R1 to Y39*GM1 overlaps with minor distance contributions in the range of 2 to 2.8 nm, in agreement with the experimentally observed low labeling efficiency of C70R1. The distance distribution of the "outer conformation" after the MD simulation is shown in Fig. 2B.

### SI 6 DEER spectroscopy on eGFP-Y39SCO*$Gd^{3+}$-DOTAM-azide-C48R1-C70R1 mutant

Echo-detected field sweep of the eGFP-Y39SCO*GDMA-C48R1-C70R1 with shot repetition times of 200000 and 1000 µs are shown in Fig. S7 and display the spectra of $Gd^{3+}$ and nitroxide with a residual signal of $Gd^{3+}$, respectively.

The DEER data were analyzed using DeerAnalysis2019 [25]. The primary and background-corrected DEER signals and corresponding distance distributions obtained by NeuralNet or Tikhonov regularization tool are shown in Fig. S8.

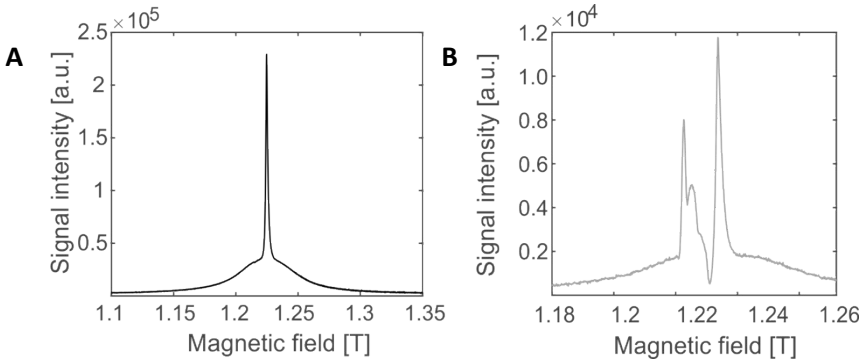


**Figure S7**. 10 K Echo-detected field sweep of eGFP-Y39SCO*GDMA-C48R1-C70R1 recorded with shot repetition times of 1000 (**A**) and 200000 µs (**B**).

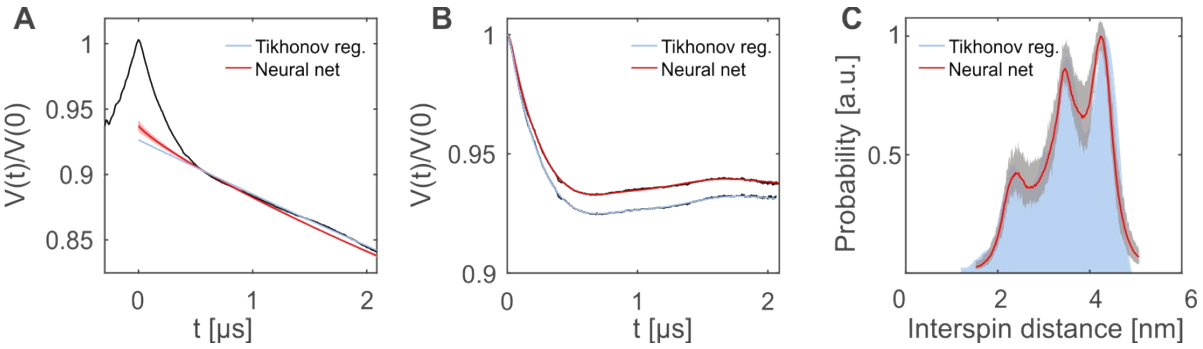


**Figure S8**. The primary (**A**), and background-corrected (**B**) DEER signal of eGFP-Y39SCO*GDMA-C48R1-C70R1 with corresponding distance distributions (**C**) obtained by Tikhonov regularization (blue) and NeuralNet tool (red) in DEERAnalysis2019.[25] Experimental data is shown in black. Fits (red and blue lines) represent the homogeneous background correction (**A**) and the form factor fit (**B**) that corresponds to the experimental distance distribution.

**SI 7 Toxicity, stability and cell penetration assays**

*Toxicity*

Toxicity of $Gd^{3+}$-DOTA(M) (GD/GDM) was examined using the agar plate method described in [26]. Briefly, an overnight culture of *E.coli BL21* cells was equally distributed as a thin layer on Agar plates and pre-incubated for 1 h at 37°C. After that, 1 µl of the compounds ($GdCl_3$, $Gd^{3+}$-DOTA(M), DOTA(M)) were put in different pre-marked segments and incubated overnight at 37°C. The diameter of segments with inhibited cell growth were measured. As can be seen from Fig. S9, *E.coli BL21* cell growth was unaffected by the presence of both $Gd^{3+}$-DOTA(M) complexes as well as free chelates in concentrations up to 50 mM, while $GdCl_3$ appeared to be more toxic. These results are in agreement with reports for $Gd^{3+}$-complexes as MRI contrast agents.[27–29]

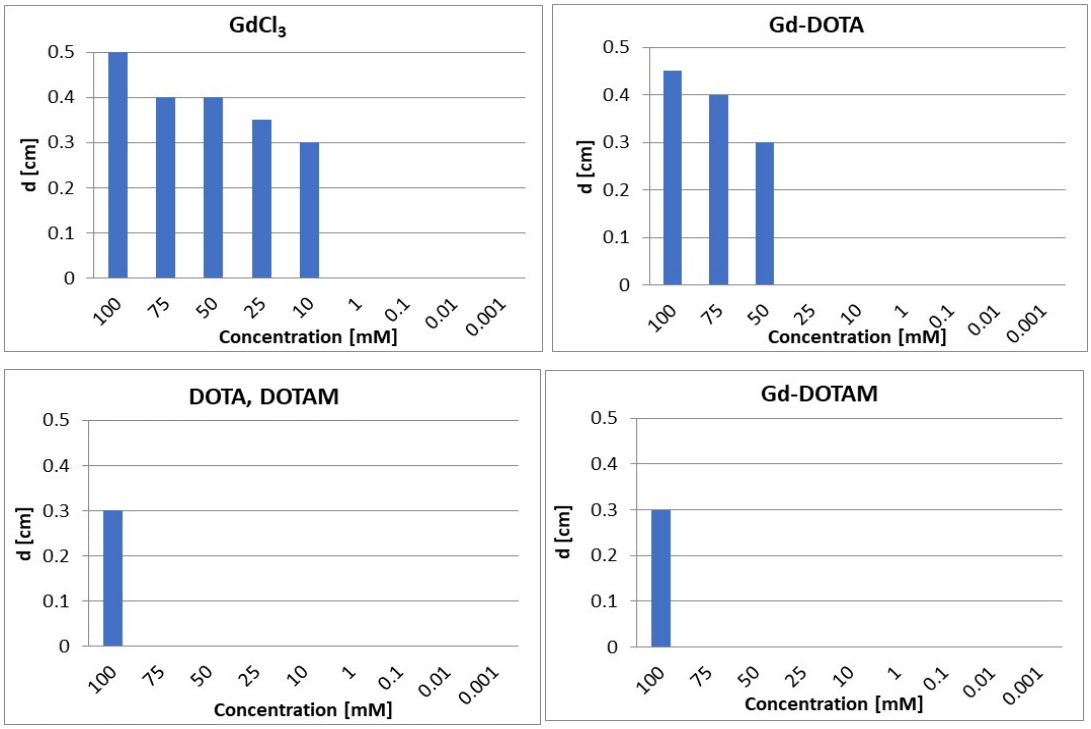


**Figure S9**. Toxicity assays of free $GdCl_3$, $Gd^{3+}$-DOTA(M), complexes and free DOTA(M). The diameter of regions with inhibited growth is shown over the concentration range from 100mM to 1µM.

*Permeability*

To test the penetration of $Gd^{3+}$ complexes with respect to *E.coli* cell membrane, complexes were added to 3 mL overnight cultures of *E.coli* $K_{12}C_{600}$ cells to a final concentration of 1 mM and incubated at 37°C while shaking in a bacterial incubator (Aerotron, Bottmingen, Switzerland) for different time intervals. Afterwards, cells were washed after 1, 3 and 9 hours incubation by exchanging the growth medium, centrifugation and resuspension and were finally concentrated to 20 µL in the capillary for the measurement. The spin concentration *C* was calculated from cw EPR spectra as described in chapter SI 2 and the spin number in the measured sample volume *V* was calculated as $N(spin)=C*N_A*V$, where $N_A$ is the Avogadro constant. The accuracy of the spin concentration determination is estimated statistically to be about ±10%.

After cw EPR measurements, the cells were collected, diluted with 4xPBS buffer (548 mM NaCl, 10.8 mM KCl, 40 mM $Na_2HPO_4$, 8 mM $KH_2PO_4$, pH 8.0) and the $OD_{600}$ was measured on an UV/VIS spectrometer 2450 (Shimadzu, Duisburg, Germany). The amount of measured cells was calculated under the assumption that the $OD_{600}$ = 1 corresponds to ~ $5*10^8$ cells/mL as found in [30].

As seen from the cw EPR spectra in Fig. S10 A, the signal amplitude of $Gd^{3+}$-DOTAM originating from *E.coli K12C600* cells increased with increasing incubation time. In contrast, the incubation of *E.coli* cells with $Gd^{3+}$-DOTA didn't result in any detectable signal since its broad linewidth limits the detection at such low concentrations at X-band. The observed line broadening with respect to free $Gd^{3+}$-DOTAM in buffer is expected due to the increased viscosity (see Fig. 1B). The spin concentration in the measured volume was estimated to be ~ 8 µM (or $4.2*10^5$ spins/cell) after 1 h incubation reaching about ~18 µM ($10.5*10^5$ spins/cell) after 9 hours of incubation. The local spin concentration inside the cell is expected to be higher since cells do not fill the whole measured volume. The determined concentrations lie in the same range as usually used for *in vivo* reactions with fluorescent dyes (10-50 µM).[31] In order to estimate the location of GDM inside the cell, cells were sonicated on ice using a standard procedure [9]. Supernatant as well as the non-water-soluble cell fraction, resuspended in buffer, were measured separately by cw EPR indicating that most of the label (~70%) was located in the soluble part of the cell lysate (see Fig. S10 B).

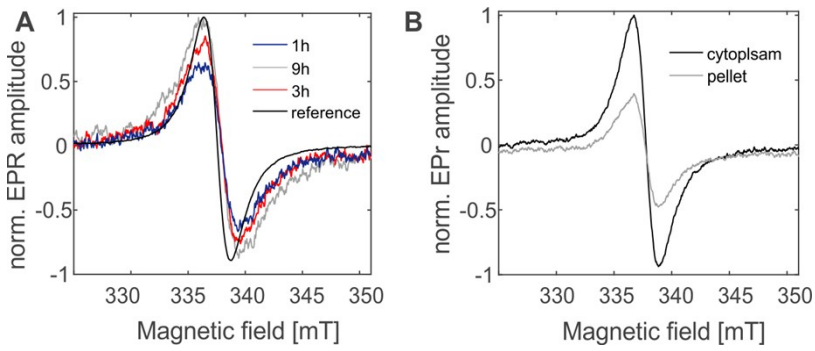


**Figure S10**. Normalized EPR spectra of washed *E.coli* $K_{12}C_{600}$ cells after A: 1 h (blue), 3 h (red) and 9 h (grey) incubation with 1 mM GDM at 37°C and B: sonification and ultracentrifugation to separate cytosolic (black) and membrane (grey) contributions. The amplitudes of the red and blue spectra in A are depicted with respect to the normalized amplitude of the grey one. 1 mM GDM in buffer is shown in A in black as a reference.

*Stability*

To test the spin label stabilities in reducing *E.coli* environment, lysate of *E.coli* $K_{12}C_{600}$ cells was prepared by sonication[6] of cells resuspended 1:1 v/v in 4xPBS buffer. Then, 20 µL of lysate was taken for each sample and mixed with a spin label to a final concentration of 4 mM. The observed deviation in starting concentration is due to the error in spin concentration determination by double integration (see SI 2). Fig. S11 presents the reduction kinetics plotted as spin concentration determined from cw EPR spectra versus incubation time for $Gd^{3+}$-DOTAM in comparison to commonly used $Gd^{3+}$-DOTA and the nitroxide radical PCA.

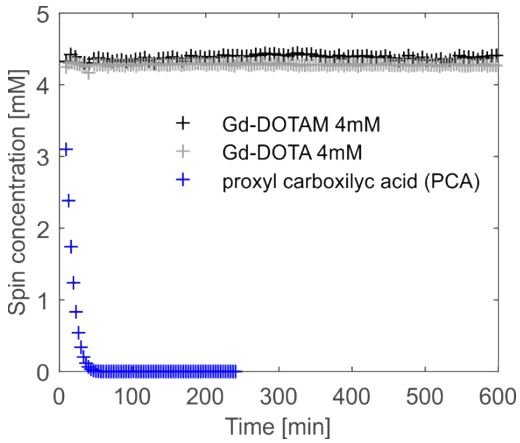


**Figure S11**. Cw EPR reduction kinetics in *E.coli* $K_{12}C_{600}$ cell lysate for 4 mM of Gd-DOTA (grey), Gd-DOTAM (black) and proxyl carboxylic acid (PCA, blue).

**SI 8 *In cell* sample preparation**

After expression of eGFP-Y39SCO, *E.coli BL21* cells were washed three times with 4xPBS buffer and resuspended in the same buffer in 1:1 v/v ratio. GDMA stock solution was added to the cell suspension to a final concentration of 1 mM and placed into an incubator (Heraeus Function Line B6, Thermo Fischer Scientific Braunschweig, Germany) for 2 h and 6 h at 37°C. After incubation cells were washed from extracellular spin label three times by resuspension on ice and centrifugation at 4°C with PBS buffer for 5 min and resuspended in the same buffer to 1:1 v/v. 40 µL of resuspended cells were placed in the capillary for the EPR measurements (see Fig. 3A). In parallel, the remaining sample was mixed with 1 mM proteinase inhibitor (PMSF, Sigma Aldrich) and 0.2 mM TCEP and sonicated on ice. The

supernatant was quickly separated by centrifugation for 5 min at 13000 rpm at 4°C and purified by filtration with a Zeba Spin (Thermo Fisher Scientific, Braunschweig, Germany) Column 10 kDa MWCO (1 min, 1000 rpm) at 4°C in order to get rid of remaining unbound spin label, and subsequently concentrated using 10kDa VivaSpin concentrator (Merck, Germany) and filled into EPR capillaries for measurements (see Fig. 3B). The time of preparation did not exceed 10 min at either 4°C or on ice, therefore the labeling reaction is not expected to proceed significantly during such short period of time according to the known slow SPAAC reaction kinetics.[9] To test the cell viability after the labeling procedure carried out as described above, the cells were placed on Petri dish and incubated overnight. As can be seen from Fig. S12, cell growth was not inhibited after labeling.

**Figure S12**. Agar plate of *E.coli Bl21* cells (with expressed eGFP-Y39SCO) incubated overnight at 37°C after 2h *in cell* labeling with GDMA.

## References


1 J. Hannant, J. H. Hedley, J. Pate, A. Walli, S. A. Farha Al-Said, M. A. Galindo, B. A. Connolly, B. R. Horrocks, A. Houlton and A. R. Pike, *Chem. Commun.*, 2010, **46**, 5870–2.
2 C. F. C. Lam, A. C. Giddens, N. Chand, V. L. Webb and B. R. Copp, *Tetrahedron*, 2012, **68**, 3187–3194.
3 A. Barge, G. Cravotto, E. Gianolio and F. Fedeli, *Contrast Media Mol. Imaging*, 2006, **1**, 184–8.
4 W. Czechtizky and P. Hamley, Eds., John Wiley & Sons, Inc, Hoboken, New Jersey, 2016.
5 L. Garbuio, E. Bordignon, E. K. Brooks, W. L. Hubbell, G. Jeschke and M. Yulikov, *J. Phys. Chem. B*, 2013, **117**, 3145–3153.
6 M. Pannier, S. Veit, A. Godt, G. Jeschke and H. W. Spiess, *J. Magn. Reson.*, 2000, **142**, 331–40.
7 Y. Polyhach, E. Bordignon, R. Tschaggelar, S. Gandra, A. Godt and G. Jeschke, *Phys. Chem. Chem. Phys.*, 2012, **14**, 10762.
8 M. Yulikov, *Electron Paramagnetic Resonance: Volume 24*, 2015, **24**, 1–31.
9 S. Kucher, S. Korneev, S. Tyagi, R. Apfelbaum, D. Grohmann, E. A. Lemke, J. P. Klare, H. J. Steinhoff and D. Klose, *J. Magn. Reson.*, 2017, **275**, 38–45.
10 S. R. McRae, C. L. Brown and G. R. Bushell, *Protein Expr. Purif.*, 2005, **41**, 121–7.
11 J. B. Segur and H. E. Oberstar, *Ind. Eng. Chem.*, 1951, **43**, 2117–2120.
12 M. D. Hanwell, D. E. Curtis, D. C. Lonie, T. Vandermeersch, E. Zurek and G. R. Hutchison, *J. Cheminformatics*.
13 A. K. Rappe, C. J. Casewit, K. S. Colwell, W. A. Goddard and W. M. Skiff, *J. Am. Chem. Soc.*, 1992, **114**, 10024–10035.
14 F. Neese, *Wiley Interdisciplinary Reviews: Computational Molecular Science*, 2012, **2**, 73–78.
15 C. van Wüllen, *J. Chem. Phys.*, 1998, **109**, 392–399.
16 Y. Polyhach, E. Bordignon and G. Jeschke, *Phys. Chem. Chem. Phys.*, 2011, **13**, 2356–2366.
17 G. Jeschke, *Protein Sci.*, 2018, **27**, 76–85.
18 J. A. J. Arpino, P. J. Rizkallah and D. D. Jones, *PLoS ONE*, 2012, **7**, e47132.
19 W. Humphrey, A. Dalke and K. Schulten, *J. Mol. Graph.*, 1996, **14**, 33–38.
20 J. C. Phillips, R. Braun, W. Wang, J. Gumbart, E. Tajkhorshid, E. Villa, C. Chipot, R. D. Skeel, L. Kalé and K. Schulten, *J. Comput. Chem.*, 2005, **26**, 1781–1802.
21 R. B. Best, X. Zhu, J. Shim, P. E. M. Lopes, J. Mittal, M. Feig and A. D. MacKerell, *J. Chem. Theory Comput.*, 2012, **8**, 3257–3273.
22 N. Reuter, H. Lin and W. Thiel, *J. Phys. Chem. B*, 2002, **106**, 6310–6321.
23 D. Sezer, J. H. Freed and B. Roux, Parametrization, *J. Phys. Chem. B*, 2008, **112**, 5755–5767.
24 D. Sezer, J. H. Freed and B. Roux, *J. Am. Chem. Soc.*, 2009, **131**, 2597–2605.
25 G. Jeschke, V. Chechik, P. Ionita, A. Godt, H. Zimmermann, J. Banham, C. R. Timmel, D. Hilger and H. Jung, *Appl. Magn. Reson.*, 2006, **30**, 473–498.
26 D. Liu and K. Kwasniewska, *Bull Environ Contam Toxicol*, 1981, **27**, 289–94.
27 P. Caravan, J. J. Ellison, T. J. McMurry and R. B. Lauffer, *Chem. Rev.*, 1999, **99**, 2293–352.
28 S. K. Morcos, *Eu. J. Radiol.*, 2008, **66**, 175–179.
29 M. Port, J.-M. Idée, C. Medina, C. Robic, M. Sabatou and C. Corot, Efficiency, *BioMetals*, 2008, **21**, 469–490.
30 G. Sezonov, D. Joseleau-Petit and R. D'Ari, *J. Bacteriol.*, 2007, **189**, 8746.
31 K. E. Beatty, F. Xie, Q. Wang and D. A. Tirrell, *J. Am. Chem. Soc.*, 2005, **127**, 14150–14151.